AMONuSeg: A Histological Dataset for African Multi-Organ Nuclei Semantic Segmentation.

Hasnae Zerouaoui[1,*], Gbenga Peter Oderinde[2,*], Rida Lefdali[1,*], Karima Echihabi[1], Stephen Peter Akpulu[3], Nosereme Abel Agbon[2], Abraham Sunday Musa[2], Yousef Yeganeh[4,5], Azade Farshad[4,5], and Nassir Navab[4,5]

[1] Mohammed VI Polytechnic University, Benguerir, Morocco
`hasnae.Zerouaoui@um6p.ma`
[2] Ahmadu Bello University, Zaria, Nigeria
[3] Federal University of Lafia, Lafia, Nigeria
[4] Technical University of Munich, Munich, Germany
[5] Munich Center for Machine Learning, Munich, Germany

Abstract. Nuclei semantic segmentation is a key component for advancing machine learning and deep learning applications in digital pathology. However, most existing segmentation models are trained and tested on high-quality data acquired with expensive equipment, such as whole slide scanners, which are not accessible to most pathologists in developing countries. These pathologists rely on low-resource data acquired with low-precision microscopes, smartphones, or digital cameras, which have different characteristics and challenges than high-resource data. Therefore, there is a gap between the state-of-the-art segmentation models and the real-world needs of low-resource settings. This work aims to bridge this gap by presenting the first fully annotated African multi-organ dataset for histopathology nuclei semantic segmentation acquired with a low-precision microscope. We also evaluate state-of-the-art segmentation models, including spectral feature extraction encoder and vision transformer-based models, and stain normalization techniques for color normalization of Hematoxylin and Eosin-stained histopathology slides. Our results provide important insights for future research on nuclei histopathology segmentation with low-resource data. Code and dataset: `https://github.com/zerouaoui/AMONUSEG` [6]

Keywords: Semantic Segmentation · Digital Pathology · Visual Transformers · Nuclei Segmentation · Spectral Features · Low-resources datasets.

1 Introduction

Haematoxylin and Eosin (H&E)-stained histopathology images are considered the gold standard in pathology for cancer diagnosis [2]. The staining process of the histopathology images enables an accurate understanding of biological structure, leading to better identification of pathological changes and, therefore,

---

[6] *H.Zerouaoui, O. Gbenga and R. Lefdali : Equal Contribution

better cancer diagnosis. In addition to that, segmentation of the nuclei of the histopathology images using deep learning (DL) models helps the pathologists confirm or refute their diagnosis and, therefore, propose a better treatment plan for their patients [2]. However, the lack of publicly available African datasets makes training models that can generalize across varied patient populations extremely difficult [12]. Furthermore, the analysis of state-of-the-art (SOTA) segmentation models using spectral feature extraction encoders and vision transformers (ViT) for nuclei histopathology segmentation can provide key insights for proposing new segmentation approaches to the digital pathology research field [10,26]. In this work, we introduce, to the best of our knowledge, the first fully annotated African multi-organ dataset acquired using low-resource equipment for nuclei semantic segmentation of three organs (breast, cervix, and skin) and one body region (inguinal lymph nodes). Further, we investigate the effect of stain-normalization techniques in three different normalization categories: (1) color deconvolution methods, (2) color transfer approaches, and (3) generative adversarial neural network (GAN)-based techniques. We assess six SOTA segmentation models, and we propose a modified model, FD-NET, by merging a spatial encoder branch and a spectral encoder branch using Fast Fourier Transformation blocks [6]. The spatial encoder branch processes an input image, while the spectral encoder branch processes the input image along with a generated mean attention map using Dino V1 [5,10,26]. In summary, the main contributions of this paper are: (1) We introduce the first fully annotated, publicly available African Multi-Organ dataset (AMONuSeg) for nuclei semantic segmentation; (2) we analyze the impact of stain color normalization techniques on the segmentation performance; (3) we assess the impact of SOTA segmentation models on nuclei histopathology segmentation; and (4) we propose a modified merged FD-NET segmentation model.

2   Related Work

Nuclei segmentation plays a key role in the analysis of H&E-stained histopathology images, yet it remains a challenging task in computer-aided analysis. DL-based methods have been actively explored for medical image segmentation. For instance, U-Net [22], an autoencoder-decoder-based model with a skip connection, achieved the best performance in the International Symposium on Biomedical Imaging (ISBI) cell tracking challenge and, thus, has become the baseline architecture for the segmentation task, especially in medical applications including nuclei segmentation [20] [18]. Most deep learning architectures use regular convolution blocks for feature extraction, which operate locally. Therefore, Lu Chi *et al.* [6] proposed the Fast Fourier Convolution Block (FFC) that focuses not only on the local receptive fields but also on learning global patterns through the spectral domain. Incorporating FFC blocks into models such as ResNet 101 or ResNet 50 [13] has shown an improvement in the performance on ImageNet compared to using those models with regular convolution blocks [10,6]. The use of FFC block in segmentation tasks has been recently explored. Farshad *et al.*

[10] proposed Y-Net, which combines a spatial encoder extracting the local features with a spectral encoder that uses FFC blocks to extract frequency domain features. Results show that Y-Net outperforms existing models in segmenting the fluid area in OCT images. Furthermore, the application of transformers in recognition tasks has demonstrated promising results. Dosovitskiy *et al.* [8] introduced Vision Transformers (ViTs), which perform better than CNN-based architectures, such as ResNet, for classification tasks. ViT divides the input image into fixed-size patches, linearly embeds them, and processes them through a multi-head attention mechanism and an MLP head to perform the classification. Caron *et al.* [5] propose DINO, a self-supervised learning method using self-distillation between two networks, both employing the ViT architecture. DINO reveals that features of self-supervised ViT capture meaningful semantic segmentation information, which is not the case with supervised ViT or CNNs. DAINet, proposed by Yeganeh *et al.* [26], leverages the semantic information encoded in the attention maps of a pre-trained DINO by employing dual encoders: one for spatial features extraction from the input image and the other for features extraction from the attention maps. DAINet shows a significant improvement in the segmentation of abdominal images of the Synapse Dataset. H&E-stained histopathology images present a color variability due to factors such as tissue type, preparation, microscope settings, or imaging quality. This color variation makes the use of histopathology images very challenging in DL-based analysis. Many methods for stain normalization, such as Macenko [19], Reinhard [23], or StainGAN [25], have been developed to reduce color variability. These methods rely on adjusting the color distribution of the source images to match that of a target template image. J. Boschman *et al.* [2] provided a comprehensive study on using stain normalization techniques in the classification. The results reveal that color normalization techniques can improve the deep learning model performance when using a dataset from multiple centers. In the case of a single center, these techniques do not consistently improve performance.

3   Method

This section describes the key contribution of this work by presenting the process of acquiring and annotating the first public fully annotated H&E-stained nuclei semantic segmentation (AMONuSeg) dataset. We also describe the stain normalization framework followed to pre-process the dataset.

3.1   AMONuSeg: African Multi-Organ Nuclei Semantic Segmentation Dataset

This paper introduces the first fully annotated H&E-stained African multi-organ for nuclei semantic segmentation dataset. The dataset contains 48 images with a size of 1280x960 and 250x Magnification Factor (MF) [7] collected using a digital microscopic camera (MA 500 AmScope Matlab ®, USA) [17]. The images

---

[7] 250x is calculated by the magnification of the eyepiece which is 10x and the objective lens which is 25x.

originating from three organs and one region (breast, cervical, skin, and inguinal lymph nodes) were carefully selected and processed by a senior pathologist. Table 1 describes the details of the AMONuSeg dataset in comparison to the three publicly available datasets CryonuSeg [20], Monuseg [18] and TNBC [21] that were acquired from The Cancer Genome Atlas (TCGA) Portal [7]. Following the completion of the sample preparation steps, which included tissue processing and H&E staining, two trained annotators conducted the annotation process. The details of the sample preparation and annotation process are described in this Section.

Table 1. Description of the three public datasets for nuclei semantic segmentation: MoNuSeg, CryoNuSeg, TNBC, and the newly collected African dataset, AMONuSeg

Dataset	#Image	Body-Part	#Nuclei	MF	Image Size	Source
MoNuSeg [18]	30	7	28,846	40x	1000x1000	TCGA
CryoNuSeg [20]	30	10	8,251	40x	512x512	TCGA
TNBC [21]	50	1	4,022	40x	512x512	TCGA
AMONuSeg (Ours)	48	4	19,036	250x	1280x960	Nigeria

Tissue Processing   Duplicated samples of surgically resected cancerous tissues were collected and fixed in neutral buffered formalin. The fixed tissues were removed from the neutral-buffered formalin and dehydrated using ascending grades of alcohol. The method involved dehydration of the tissues in two changes of 70% alcohol, two changes of 90% alcohol, three changes of 95% alcohol, and three changes of absolute alcohol. Each stage lasted for 30 minutes. The dehydrated tissues were cleared with two changes of chloroform for two hours. The cleared tissues were infiltrated by immersing them in molten paraffin wax and then allowed to solidify. The embedded tissues were encased in a rectangular block and then used with a rotary microtome at 5 µm per section [24]. The tissue sections were floated out in a water bath at 30°C, and clean slides were used to pick up the tissues from the warm water bath. The tissues were then stained using the H&E-staining method.

Haematoxylin and Eosin (H and E) staining method   The method of H&E staining was carried out by dewaxing the tissue in two changes of xylene for three minutes each, hydrated by passing them through descending grades of alcohol (100%, 95%, 90%, and 70%) for three minutes each, then stained in hematoxylin for ten minutes, and washed in tap water to remove excess stain. The slides were then flooded with acid alcohol for a few seconds for differentiation and then washed in tap water again. The slides were then placed in Scott's tap water for five minutes and counter-stained with Eosin for three minutes. The sections were rinsed in tap water, dehydrated in ascending grades of alcohol, and cleared in xylene. The sections were then covered using a mountant [24].
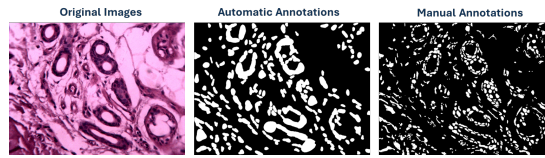
Fig. 1. The difference between automatic annotations generated using the Fiji ImageJ where the nuclei are merged and the manual annotations of samples of a histopathology breast image .

Annotation Process   Two trained annotators, a data scientist (A1) and a post-doc researcher (A2), conducted the annotation process on nuclei segmentation by an expert pathologist to generate the ground truth masks. The annotation protocol was inspired by the CryoNuSeg and MoNuSeg datasets protocols [20,18], which was further enhanced by adding a first validation using the masks generated automatically by the FIJI ImageJ software [9]. Below is a detailed description of the annotation process:

1. Generate unsupervised automatic nuclei semantic segmentation masks using the Fiji ImageJ software [9], which serve as preliminary annotations for the tissue slides. These annotations provide a rough estimate of the nuclei locations, simplifying the initial annotation process for the two annotators A1 & A2.
2. Perform manual nuclei semantic segmentation using the LabelStudio [4] segmentation tool by the two annotators A1 & A2.
3. Conduct a second round of intra-observation by A2 to validate the annotations made by A1.
4. Validate the final manual-generated ground truth masks by three expert pathologists with 4, 10 and 15 years of experience.
5. Correct the manual nuclei annotations based on the mark-ups and observations of the three expert pathologists.
6. Conduct a final validation by three expert pathologists to ensure that the annotations meet the highest standards to help the pathologist make the diagnosis. [8]

A visualization of automatic segmentation using Fiji ImageJ compared to manual segmentation is presented in Figure 1.

3.2   Stain Normalization

One of the biggest challenges in the application of segmentation models for the digital pathology of H&E-stained samples is the color variations of (1) the staining process using the H&E stains [3] and (2) the different scanners used

---

[8] Due to disagreements among pathologists [20], in this paper, we present annotations validated by three expert pathologists where they reached agreements.
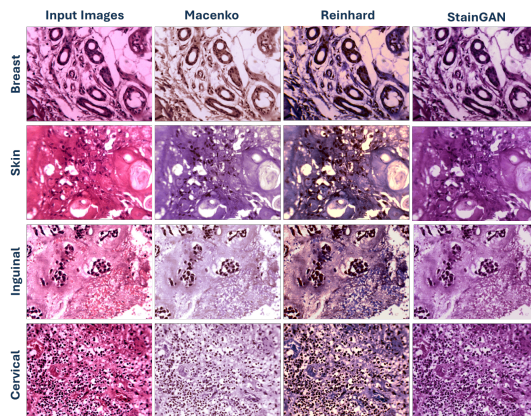
Fig. 2. AMONuSeg input images of the three organs (breast, skin, and cervix) and inguinal region, along with their corresponding processed stain normalized images using Macenko, Reinhard, and StainGAN approaches.

to digitize the whole slide images tissues [16]. A number of stain normalization techniques have been proposed to reduce the variability of colors in the H&E-stained histology images. These approaches can be divided into three categories, including (1) color deconvolution methods that involve segregating the colors into their staining components before applying the transformation [19], (2) color transfer approaches that adjust the color of an input image to match that of a target image [23], and (3) generative adversarial neural network (GANs) based techniques that leverage adversarial training to learn mappings between different stain spaces, allowing for the adaptation of images to a standardized stain appearance [25]. In this study, we used Macenko [19], Reinhard [23], and Stain-GAN techniques [25], each of which corresponds to one of the aforementioned approaches, respectively, to evaluate their impact as a pre-processing technique for histopathology nuclei image segmentation. Figure 2 illustrates samples from different body organs and regions, with different stain normalization approaches.

4   Experiments

In this section, we summarize the results of the experimental evaluation conducted on the proposed AMONuSeg dataset. We present the experimental setup, discuss the results of the assessed segmentation models, and conduct an ablation study of the FD-NET proposed model [10] to analyze the impact of spectral features encoder branch and ViT [8] on the segmentation task.

4.1   Experimental Setup

The experimental protocol followed to evaluate the SOTA methods is the same as prior works [20]. The AMONuSeg dataset consists of H&E-stained histopathol-

ogy images of three organs and one body region with 12 images per organ. A 3-fold cross-validation was performed to evaluate the models, with each fold comprising 36 images for training and 12 images for validation. All the models except DAINet [26] were trained with a batch size of 8, a learning rate of 1e-4, the Adam optimizer [26], and a maximum of 400 epochs. As for the DAINet model, DINO V1 [5] was retrained using the PanNuke dataset [11], which contains 7000 H&E-stained histopathology images, and ViT-S/16 model with a batch size of 64 and a learning rate of 1e-4. For the augmentation of the AMONuSeg dataset, we applied random transformations, including horizontal flip, vertical flip, and rotations. As for the training, we dispatched the images to patches of size 512x512 and therefore increased the image samples from 48 images of size 1280x960 to 348 patches of size 512x512. The patches are then resized to 256x256. We report the average Dice score [10,26,14] of all the evaluated models. All experiments were run using an NVIDIA A100-SXM4-80GB GPU.

4.2   Results

Table 2 describes the results of the average Dice score of the selected segmentation models when applied to the original images of the AMONuSeg dataset and its pre-processed variants using the three stain normalization techniques Macenko [19], Reinhard [23], and StainGAN [25]. It is observed that the stain normalization techniques used have a minor impact on the performance prior to the original dataset with a tendency of achieving minor improvement in terms of the average Dice score when using the StainGAN approach [25]. The lack of a consistent best stain normalization technique suggests that these methods do not impact the segmentation performance. Furthermore, we noticed that most of the SOTA models did not outperform the baseline U-Net for nuclei histopathology segmentation. Although transformer-based and spectral feature extraction encoder-based models show significant improvement in other medical modalities such as optical coherence tomography [10] and computed tomography images [26], the challenge of accurately segmenting small objects, such as the nuclei, remains a significant bottleneck limiting performance improvements over U-Net in the H&E-stained histopathology image segmentation task [15].

Ablation Study The last row of Table 2 presents an ablation study of the Y-Net model [10] components. We opted to modify the Y-Net model due to its comparable performance with the baseline U-Net for nuclei segmentation by merging it with the DAINet model [26]. Y-Net consists of two encoder branches using the same spatial encoder used in U-Net with regular convolution blocks in the first branch and a spectral encoder in the second branch using the FFC blocks [6]. Alternatively, the DAINet model consists of two convolution encoder branches, one using the original images as input and a second using the attention maps generated using DINO V1 [5]. In order to study the impact of both spectral encoders and ViT-based segmentation, we changed the input images of Y-Net components by feeding the FFC branch with both the original input images and
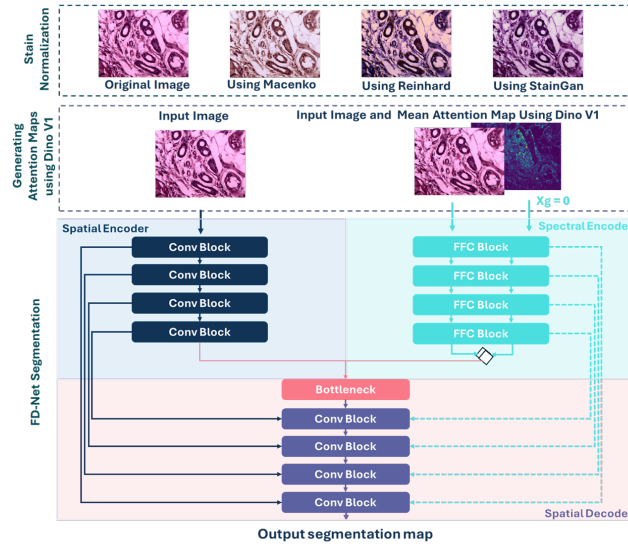
Fig. 3. FD-Net: The proposed network [10] has two branches: (1) Spatial encoder branch that processes spatial features and consists of convolutional blocks (Convolutional layer, batch normalization layer, a ReLU activation function, and a max pooling layer) and (2) Spectral branch that processes spectral features and consists of fast Fourier convolutional blocks [6]. An input image, which can be either the original image or a stain-normalized preprocessed image using Macenko, Reinhard, or StainGAN methods, is fed to the spatial encoder branch, while the input image and the generated mean attention map using Dino v1 are fed to the spectral branch.

the mean attention maps generated using DINO V1 and the original input in the spatial encoder branch as illustrated in Figure 3. As a result, the modified Y-Net named FD-NET did not show a significant improvement in terms of the average Dice score but achieved competitive performance compared to SOTA models [15]. We believe that, despite the staining specificity of the H&E-stained histopathology images, the particularity of the small size of the nuclei may not align effectively, leading to non-significant improvement of the performance even while using ViT-based models and spectral feature extraction encoder branches.

4.3   Discussion and Conclusion

In this study, we introduced the first fully annotated AMONuSeg public dataset for nuclei semantic segmentation that offers 48 H&E-stained histopathology images using the 250X MF and the size of 1280x960 of three organs (breast, cervix, and skin) and one region (inguinal lymph nodes) acquired using limited resources. We also analyze the impact of both stain normalization techniques and SOTA segmentation models, particularly the ones integrating spectral encoder

Table 2. The average Dice score of the evaluated segmentation models on the Original and pre-processed AMONuSeg dataset using the Stain-Normalization techniques .

Model	Original Dataset	Preprocessing		
		Macenko [19]	Reinhard [23]	StainGAN [25]
U-Net [22]	0.823	0.794	**0.825**	0.826
SegNet [1]	0.809	0.755	0.799	0.809
Y-Net [10]	**0.830**	0.794	0.825	0.826
DAINet [26]	0.824	0.793	0.822	0.828
TransNuseg [14]	0.815	0.791	0.814	0.813
FD-Net	0.828	**0.796**	0.822	**0.830**

branches and ViT-based segmentation models. We hypothesize that the stain of the histopathology images represents spectral features that can be extracted more effectively using an FFC [6] based model and that the segmentation performance can be improved using ViT [8] models such as DINO V1. Therefore, we compared our proposed model FD-Net to the SOTA baselines: Y-Net [10], DAINet [26], TransNuseg [14], U-Net [22], and SegNet [1]. In this evaluation, we used the original AMONuSeg dataset, and its variants stain normalized with Macenko [19], Reinhard [23] and StainGAN [25]. Results showed that nuclei segmentation remains a challenging problem: despite the novelty of the proposed approach and the use of stain normalization techniques, minor improvements in terms of performance were reported compared to the baseline U-Net. The best performance achieved a higher average Dice score of 0.83 using both Y-Net with the original AMONuSeg and FD-Net with the StainGAN pre-processed dataset. In conclusion, our findings suggest that despite employing stain normalization techniques, spectral feature extraction encoder, and ViT-based models, the segmentation of nuclei was not be improved due to the different levels of granularity [15] and the small size of nuclei in H&E-stained histopathology images.

References

1. Vijay Badrinarayanan, Alex Kendall, and Roberto Cipolla. Segnet: A deep convolutional encoder-decoder architecture for image segmentation. *IEEE transactions on pattern analysis and machine intelligence*, 39(12):2481–2495, 2017.

2. Jeffrey Boschman, Hossein Farahani, Amirali Darbandsari, Pouya Ahmadvand, Ashley Van Spankeren, David Farnell, Adrian B Levine, Julia R Naso, Andrew Churg, Steven JM Jones, et al. The utility of color normalization for ai-based diagnosis of hematoxylin and eosin-stained pathology images. *The Journal of Pathology*, 256(1):15–24, 2022.
3. Jeffrey Boschman, Hossein Farahani, Amirali Darbandsari, Pouya Ahmadvand, Ashley Van Spankeren, David Farnell, Adrian B Levine, Julia R Naso, Andrew Churg, Steven JM Jones, et al. The utility of color normalization for ai-based diagnosis of hematoxylin and eosin-stained pathology images. *The Journal of Pathology*, 256(1):15–24, 2022.
4. Gustavo Carneiro, Diana Mateus, Loïc Peter, Andrew Bradley, João Manuel RS Tavares, Vasileios Belagiannis, João Paulo Papa, Jacinto C Nascimento, Marco Loog, Zhi Lu, et al. *Deep Learning and Data Labeling for Medical Applications: First International Workshop, LABELS 2016, and Second International Workshop, DLMIA 2016, Held in Conjunction with MICCAI 2016, Athens, Greece, October 21, 2016, Proceedings*, volume 10008. Springer, 2016.
5. Mathilde Caron, Hugo Touvron, Ishan Misra, Hervé Jégou, Julien Mairal, Piotr Bojanowski, and Armand Joulin. Emerging properties in self-supervised vision transformers. In *Proceedings of the IEEE/CVF international conference on computer vision*, pages 9650–9660, 2021.
6. Lu Chi, Borui Jiang, and Yadong Mu. Fast fourier convolution. *Advances in Neural Information Processing Systems*, 33:4479–4488, 2020.
7. Mario Deng, Johannes Brägelmann, Joachim L Schultze, and Sven Perner. Web-tcga: an online platform for integrated analysis of molecular cancer data sets. *BMC bioinformatics*, 17:1–7, 2016.
8. Alexey Dosovitskiy, Lucas Beyer, Alexander Kolesnikov, Dirk Weissenborn, Xiaohua Zhai, Thomas Unterthiner, Mostafa Dehghani, Matthias Minderer, Georg Heigold, Sylvain Gelly, et al. An image is worth 16x16 words: Transformers for image recognition at scale. *arXiv preprint arXiv:2010.11929*, 2020.
9. Lucas Encarnacion-Rivera, Steven Foltz, H Criss Hartzell, and Hyojung Choo. Myosoft: an automated muscle histology analysis tool using machine learning algorithm utilizing fiji/imagej software. *PloS one*, 15(3):e0229041, 2020.
10. Azade Farshad, Yousef Yeganeh, Peter Gehlbach, and Nassir Navab. Y-net: A spatiospectral dual-encoder network for medical image segmentation. In *International Conference on Medical Image Computing and Computer-Assisted Intervention*, pages 582–592. Springer, 2022.
11. Jevgenij Gamper, Navid Alemi Koohbanani, Ksenija Benet, Ali Khuram, and Nasir Rajpoot. Pannuke: an open pan-cancer histology dataset for nuclei instance segmentation and classification. In *Digital Pathology: 15th European Congress, ECDP 2019, Warwick, UK, April 10–13, 2019, Proceedings 15*, pages 11–19. Springer, 2019.
12. Lidia Garrucho, Kaisar Kushibar, Socayna Jouide, Oliver Diaz, Laura Igual, and Karim Lekadir. Domain generalization in deep learning based mass detection in mammography: A large-scale multi-center study. *Artificial Intelligence in Medicine*, 132:102386, 2022.
13. Kaiming He, Xiangyu Zhang, Shaoqing Ren, and Jian Sun. Deep residual learning for image recognition, 2015.
14. Zhenqi He, Mathias Unberath, Jing Ke, and Yiqing Shen. Transnuseg: A lightweight multi-task transformer for nuclei segmentation. In *International Conference on Medical Image Computing and Computer-Assisted Intervention*, pages 206–215. Springer, 2023.

15. Dinkar Juyal, Harshith Padigela, Chintan Shah, Daniel Shenker, Natalia Harguin-deguy, Yi Liu, Blake Martin, Yibo Zhang, Michael Nercessian, Miles Markey, Isaac Finberg, Kelsey Luu, Daniel Borders, Syed Ashar Javed, Emma Krause, Raymond Biju, Aashish Sood, Allen Ma, Jackson Nyman, John Shamshoian, Guillaume Chhor, Darpan Sanghavi, Marc Thibault, Limin Yu, Fedaa Najdawi, Jennifer A. Hipp, Darren Fahy, Benjamin Glass, Eric Walk, John Abel, Harsha Pokkalla, Andrew H. Beck, and Sean Grullon. Pluto: Pathology-universal transformer, 2024.
16. Amjad Khan, Andrew Janowczyk, Felix Müller, Annika Blank, Huu Giao Nguyen, Christian Abbet, Linda Studer, Alessandro Lugli, Heather Dawson, Jean-Philippe Thiran, et al. Impact of scanner variability on lymph node segmentation in computational pathology. *Journal of pathology informatics*, 13:100127, 2022.
17. Antje Kilias, Andres Canales, Ulrich P Froriep, Seongjun Park, Ulrich Egert, and Polina Anikeeva. Optogenetic entrainment of neural oscillations with hybrid fiber probes. *Journal of neural engineering*, 15(5):056006, 2018.
18. Neeraj Kumar, Ruchika Verma, Deepak Anand, Yanning Zhou, Omer Fahri Onder, Efstratios Tsougenis, Hao Chen, Pheng-Ann Heng, Jiahui Li, Zhiqiang Hu, et al. A multi-organ nucleus segmentation challenge. *IEEE transactions on medical imaging*, 39(5):1380–1391, 2019.
19. Marc Macenko, Marc Niethammer, James S Marron, David Borland, John T Woosley, Xiaojun Guan, Charles Schmitt, and Nancy E Thomas. A method for normalizing histology slides for quantitative analysis. In *2009 IEEE international symposium on biomedical imaging: from nano to macro*, pages 1107–1110. IEEE, 2009.
20. Amirreza Mahbod, Gerald Schaefer, Benjamin Bancher, Christine Löw, Georg Dorffner, Rupert Ecker, and Isabella Ellinger. Cryonuseg: A dataset for nuclei instance segmentation of cryosectioned h&e-stained histological images. *Computers in biology and medicine*, 132:104349, 2021.
21. Peter Naylor, Marick Laé, Fabien Reyal, and Thomas Walter. Segmentation of nuclei in histopathology images by deep regression of the distance map. *IEEE transactions on medical imaging*, 38(2):448–459, 2018.
22. Olaf Ronneberger, Philipp Fischer, and Thomas Brox. U-net: Convolutional networks for biomedical image segmentation. In *Medical Image Computing and Computer-Assisted Intervention–MICCAI 2015: 18th International Conference, Munich, Germany, October 5-9, 2015, Proceedings, Part III 18*, pages 234–241. Springer, 2015.
23. Santanu Roy, Shubhajit Panda, and Mahesh Jangid. Modified reinhard algorithm for color normalization of colorectal cancer histopathology images. In *2021 29th European Signal Processing Conference (EUSIPCO)*, pages 1231–1235. IEEE, 2021.
24. P Senthamil Selvan, S Ushakumary, and Geetha Ramesh. Studies on the histochemistry of the proventriculus and gizzard of post-hatch guinea fowl numida meleagris. *Int. J. Poult. Sci*, 7(11):1112–1116, 2008.
25. M Tarek Shaban, Christoph Baur, Nassir Navab, and Shadi Albarqouni. Staingan: Stain style transfer for digital histological images. In *2019 Ieee 16th international symposium on biomedical imaging (Isbi 2019)*, pages 953–956. IEEE, 2019.
26. Yousef Yeganeh, Azade Farshad, Peter Weinberger, Seyed-Ahmad Ahmadi, Ehsan Adeli, and Nassir Navab. Transformers pay attention to convolutions leveraging emerging properties of vits by dual attention-image network. In *Proceedings of the IEEE/CVF International Conference on Computer Vision*, pages 2304–2315, 2023.